

Low-Energy Electron Beam Dosimetry

M. R. Cleland, R. A. Galloway, T. F. Lisanti
IBA Industrial, Inc.
Edgewood, NY 11717, USA

Abstract

A determination of absorbed dose can be derived from Monte Carlo calculations of the energy deposition per electron in thin layers of any material. The data needed for the input files are accelerating voltage or incident electron energy, electron beam current, atomic composition, thickness and density of the electron beam window material, the air space, the irradiated material, its web width and line speed and the supporting material. Corrections can be applied to account for the loss of beam current due to a window support grid and from excessive beam width. The sensitivity of the results to variations in these quantities can be evaluated by repeating the calculations with different input values. Such analyses can also be applied to thin-film dosimeters and their backing materials. The ratio of the surface dose to the average dose can be determined from a depth-dose distribution curve whenever the penetration of a low-energy beam is too shallow to deliver a uniform dose within a dosimeter, which was calibrated using radiation with greater penetration. An equation for absorbed dose vs beam current, line speed and web width can be used with flat sheets or webs to compute the proportionality factor “k”, which is called the machine yield. This factor can also be determined with appropriate dosimetry.

Introduction

Monte Carlo calculations of the energy deposition per incident electron in irradiated materials can provide useful information about the capabilities and limitations of a proposed irradiation process. This method of analysis can be more convenient than dose measurement when suitable equipment is not readily available or when the available equipment does not have the operational capabilities needed for the proposed process. There are examples of such calculations in previous publications¹⁻⁸. An earlier paper shows a variety of depth-dose distributions in flat polyethylene sheets irradiated with high-energy electrons in the range from 0.4 MeV to 10 MeV³. A more recent paper provides depth-dose distributions in flat polyethylene films irradiated with low-energy electrons in the range from 75 keV to 600 keV⁷. The results presented here provide additional insight about such depth-dose distributions in the energy range from 100 keV to 300 keV. The derivation in the following section shows how the absorbed dose in thin layers of irradiated material can be obtained from the calculated energy deposition per electron.

Derivation of the Absorbed Dose Equation

The recommended unit of absorbed dose in the International System of Units (SI) is the gray (Gy), which is defined as one joule of energy absorbed per kilogram of mass (J/kg)⁹. For industrial radiation processing, the unit more often used is the kilogray (kGy), which is one kilojoule per kilogram (kJ/kg) or one joule per gram (J/g). A joule is equivalent to one watt of power absorbed for one second (W·s). The absorbed dose D (kGy) in any material irradiated with an electron beam is proportional to the energy deposition per unit areal (or area) density of material D(e) (MeV/(g/cm²)) or (MeV·cm²/g) per

incident electron. MeV is the symbol for million electron volts. $D(e)$ can be calculated with a suitable Monte Carlo code¹⁰ for any material whose atomic composition, thickness and density are known, and for electron energies that extend from one thousand electron volts (keV) to one thousand million electron volts (GeV), which is a much greater energy than would ever be used for radiation processing. An equation relating D (kGy) and $D(e)$ for a flat sheet of material passing through a wide, uniform electron beam can be derived as follows⁵:

$$D \text{ (kGy)} = \text{Absorbed Energy (J)} / \text{Mass (g)} \quad (1)$$

The quantities listed below can be substituted in Equation (1):

Absorbed Energy (J) = Energy Absorbed per Electron x Number of Incident Electrons

The Energy Absorbed per Electron = $D(e)$ (MeV·cm²/g) x Areal Density x e x 10⁶

The Areal Density Z (g/cm²) is the mass per unit area of a thin layer of irradiated material.

The quantity, $e = 1.602 \times 10^{-19}$, is the conversion factor from one electron volt to one joule.

The same quantity, $e = 1.602 \times 10^{-19}$, is also the electrical charge in coulombs on one electron.

The Number of Incident Electrons = I (A) x T (s) / e , where I (A) is the electron beam current in amperes and T (s) is the irradiation time in seconds.

The factor $F(i)$ is the fraction of incident beam current intercepted by the irradiated material.

The Mass (g) = Z (g/cm²) x A (cm²) of a thin layer of irradiated material is given by the areal density times the area of the irradiated material.

Then Equation (1) becomes:

$$D \text{ (kGy)} = D(e) Z e 10^6 F(i) I T / (e Z A) \quad (2)$$

The quantities e and Z appear in both the numerator and the denominator and can be cancelled. Then Equation (2) can be simplified to the following form:

$$D \text{ (kGy)} = D(e) F(i) I T 10^6 / A \quad (3)$$

where $D(e)$ is in MeV·cm²/g, I is in amperes, T is in seconds and A is in square centimeters. Changing the beam current to milliamperes, the irradiation time to minutes and the material area to square meters, gives the following form:

$$D \text{ (kGy)} = 6 D(e) F(i) I T / A \quad (4)$$

Equation (4) can be rearranged as follows:

$$D \text{ (kGy)} = 6 D(e) F(i) I / (A / T) \quad (5)$$

where the quantity, A / T , is the area throughput rate of the irradiated material in square meters per minute. For a flat sheet of material passing through a uniform electron beam, A / T can be replaced with $W S$, where W is the width of the material in meters and S is the transit speed of the material in meters per minute. Then Equation (5) can be changed to the following form:

$$D \text{ (kGy)} = 6 D(e) F(i) I / (W S) \quad (6)$$

Equation (6) can be rearranged to calculate the transit speed, S, as follows:

$$S = (6 D(e) F(i) / W) I / D \text{ (kGy)} \quad (7)$$

$$S = k I \text{ (mA)} / D \text{ (kGy)} \quad (8)$$

The factor, $k = 6 D(e) F(i) / W$, may be called the Speed or Linear Processing Coefficient. In common industrial usage, it is called the Machine Yield¹¹. It is directly proportional to the energy deposition per electron and the fraction of beam current intercepted by the irradiated material and inversely proportional to the width of the irradiated material.

The accuracy of Equation (6) has been verified experimentally with an uncertainty of less than 10 percent in the electron energy range from 1.0 MeV to 10 MeV⁶. Similar benchmarking tests at lower energies have not been reported, but there is no indication that this equation would not be reliable down to an electron energy of 0.1 MeV (100 keV) or even less. Some sources of uncertainty in calculating the value of D(e) would be the composition and thickness of the electron beam window, and the thickness and density of the air between the beam window and the irradiated material. The air would be heated during a continuous irradiation process and its temperature and density would depend on the electron beam current and the flow rate of the air (or nitrogen) which is used to cool the beam window. The effects of these uncertainties can be evaluated by calculating D(e) with slightly different values for the window thickness and the air density. Examples are given in the last section of this paper.

Monte Carlo Calculations for Polyethylene

Energy Dependence of the Depth Dose Curves

The depth-dose curves presented in Figs. 1 and 2 have been calculated with the one-dimensional TIGER version of the ITS3 Monte Carlo code¹⁰. They show how the values of D(e) depend on the energy of the incident electrons and the depth in flat sheets of high-density polyethylene (HDPE). The energy deposition values are shown for a 15 μm titanium beam window and a 2.5 cm air space in front of a sheet polyethylene. The areas under these curves have the dimensions of MeV per electron, so they indicate the relative amounts of energy absorbed by each material. Such curves are often called depth-dose distributions, because D(e) is proportional to dose, according to Equations (2) through (6) in the previous section. However, D(e) does not have the units of dose. The beam current and the area throughput rate must be included to obtain dose in kGy units. Even so, such curves provide insight regarding the variations in dose that can be obtained by irradiating materials with accelerated electron beams.

Some useful features of these curves are shown in Fig. 3. The curve labeled Entrance Dose has a maximum value of 7.90 MeV cm^2/g at the incident electron energy of 150 keV. This curve decreases gradually with higher electron energies because of reduced electron stopping power. It decreases more abruptly with lower energies, because then the energy depositions in the titanium window and the air space take larger fractions of the incident energy¹¹. According to Equation (7), these characteristics mean that the transit speed would have the maximum value at 150 keV for a given beam current. The

curve labeled R(50e) Depth shows the depth where the dose equals half the entrance dose. When flat materials are irradiated from opposite sides, a thickness of twice this value will absorb a nearly uniform dose. The R(50e) Depth is only 0.0020 g/cm^2 ($21.2 \text{ }\mu\text{m}$ with a density of 0.95 g/cm^3) at 100 keV, but it increases to 0.0511 g/cm^2 ($538 \text{ }\mu\text{m}$ or 0.538 mm with a density of 0.95 g/cm^3) at 300 keV. The Absorbed Energy curve (energy absorbed in the polyethylene) is only 12.0 percent at 100 keV, but it increases to 87.7 percent at 300 keV. This quantity would be useful when calculating the average dose in fluid streams.

Similar curves shown in Fig. 4 have been calculated with a $15 \text{ }\mu\text{m}$ titanium beam window and a 5.0 cm air space⁷. It can be seen that the increased air space gives slightly different results. The Entrance Dose peaks with an incident electron energy of 175 keV instead of 150 keV, and the maximum value is slightly lower, $7.37 \text{ MeV cm}^2/\text{g}$ instead of $7.90 \text{ MeV cm}^2/\text{g}$. The values of R(50e) Depth and Absorbed Energy are also slightly lower. The R(50e) Depth is only 0.00114 g/cm^2 ($12.0 \text{ }\mu\text{m}$ with a density of 0.95 g/cm^3) at 100 keV, but it increases to 0.0474 g/cm^2 ($499 \text{ }\mu\text{m}$ or 0.499 mm with a density of 0.95 g/cm^3) at 300 keV. The Absorbed Energy curve (energy absorbed in the polyethylene) is only 2.7 percent at 100 keV, but it increases to 83.5 percent at 300 keV.

Effects of Substantially Increasing the Air Space

The effects of substantially increasing the air space between a $15 \text{ }\mu\text{m}$ titanium beam window and a thick polyethylene sheet with an incident electron energy of 200 keV are shown in Fig. 5. These depth-dose curves show the effects of increasing the air space in equal steps from 5 cm to 25 cm. Such large air spaces would not usually be used when irradiating flat materials, but they are pertinent for sterilizing three-dimensional objects, such as the surfaces of containers for medical products and foods¹. The variation in surface dose from the top to the bottom of a large, empty container can be estimated with similar, one-dimensional calculations, although a three-dimensional Monte Carlo code, such as the ACCEPT version of ITS3¹⁰, would provide more accurate information.

The first curve with an air space of 5 cm is nearly the same as the 200 keV curves in Figs. 1 and 2 with an air space of 2.5 cm. As in those curves, the first part of the curve shows the D(e) values in the titanium beam window, the second part shows the D(e) values in the air space and the rest of the curve shows the D(e) values in the polyethylene. The surface values of D(e) in the thick polyethylene sheet decrease as the air space increases, although these values are slightly higher than the corresponding depth-dose values for polyethylene shown in the first curve for 5 cm of air. The value of R(50e) Depth at 200 keV in Fig. 4, 0.0182 g/cm^2 ($192 \text{ }\mu\text{m}$ or 0.192 mm with a density of 0.95 g/cm^3), is nearly the same as the R(50e) Depth in Fig. 5.

Effects of a Stainless Steel Supporting Plate

The effects of placing a stainless steel plate underneath or behind a thin polyethylene sheet with an incident electron energy of 200 keV are shown in Fig. 6. These depth-dose curves show the effects of increasing the thickness of the polyethylene sheet in equal steps from $50 \text{ }\mu\text{m}$ to $250 \text{ }\mu\text{m}$ (0.050 mm to 0.250 mm). Electron backscattering from the stainless steel plate causes both the entrance and the exit values of D(e) in the $50 \text{ }\mu\text{m}$ and $100 \text{ }\mu\text{m}$ polyethylene sheets to increase in comparison with the 200 keV depth-dose curves in Figs. 1 and 2. The entrance values of D(e) in the 150, 200 and $250 \text{ }\mu\text{m}$ sheets are nearly the same as those in the 200 keV depth-dose curves in Figs. 1 and 2. This indicates the reduced

energy and range of the backscattered electrons, which cannot return to the entrance surface in these thicker sheets. However, the exit values of $D(e)$ in the 150, 200 and 250 μm sheets are all higher than those corresponding to the depth-dose values in Figs. 1 and 2 for 200 keV electrons in polyethylene. These backscattering effects must be taken into account when designing an irradiation process for thin plastic films.

Determination of the Low-Energy Surface Dose

Determination of the absorbed dose at or near the surface of materials irradiated with low-energy electrons is needed for regulated applications, such as sterilizing the surfaces of containers for medical products and foods. This information would also be useful, although not as important, for curing inks, coatings and adhesives on thin plastic films. When the absorbed dose within the dosimeter decreases with depth because its thickness is comparable to or even greater than the short range of the electrons, then a correction factor must be applied to the average dose reading to obtain the surface dose value⁸.

The appropriate correction factor can be obtained from a Monte Carlo calculation of the energy deposition per electron vs the areal density, as shown in the examples of Figs. 7, 8, 9 and 10, where the incident electron energies are 100, 150, 200 and 250 keV, respectively. In each case, the thickness of the electron beam window is 15 μm of titanium, the air space is 5.0 cm, the nylon dosimeter film is 50 μm and the material supporting the dosimeter is a polyethylene film thick enough to absorb the rest of the electron energy. The nylon dosimeter has been subdivided into 50 layers, each 1 μm thick, so that the absorbed dose in the first micron can be calculated. The correction factor is obtained by dividing the rectangular area, which is the product of the energy deposition per electron at the entrance surface of the dosimeter film and the areal density of the dosimeter film, by the area under the energy deposition curve within the dosimeter. The rectangular area represents the dosimeter response to penetrating radiation.

With the thicknesses of materials as assumed above, the energy deposition curve (depth-dose distribution) shown in Fig. 7 for an electron energy of 100 keV, illustrates a situation in which the electrons cannot penetrate the dosimeter film. In this case, the ratio of the surface dose to the average dose within the nylon dosimeter is 3.92. The distribution in Fig. 8 for 150 keV shows that electrons of this energy can penetrate the dosimeter, but the dose within the dosimeter is severely attenuated. The correction factor to obtain the surface dose has been reduced to 1.23. The distribution in Fig. 9 for 200 keV shows that the dose within the dosimeter is still slightly attenuated, and the correction factor is only 1.08. The distribution in Fig. 10 for 250 keV shows that the dose within the dosimeter is nearly uniform. However, the energy deposition in the first micron of the dosimeter is about 4 percent higher than it is within the rest of the dosimeter. This surface enhancement is also noticeable in Figs. 8 and 9 and also in Figs. 1 and 2, where the first point in the polyethylene portion of the depth-dose distribution curve is slightly higher than the following point. If this surface enhancement is a real effect, it might be caused by the change in atomic composition and density at the interface between different materials. Whatever the cause, it would be difficult to measure, because the thickness of the thinnest commercial dosimeters is about 10 μm .

Evaluation of Uncertainties in Monte Carlo Calculations

The accuracy of a surface dose determination using a Monte Carlo calculation depends on how well the areal densities (thicknesses and volume densities) of the beam window and the air space are

known. The window thickness can be measured before it is installed, but not after the accelerator is evacuated and ready for operation. The thickness of the air space between the window and the irradiated material can be measured, but the density of the air will depend on its temperature, which will depend on the beam current and the flow rate of the air used to cool the window and remove the ozone. So, the areal density of the air will depend on the operating conditions.

Table 1 gives comparisons of the surface values of the energy depositions per electron with two different window thicknesses. In one case, the window is 15 μm of titanium and in the other case, the window is 12 μm of titanium, a 20 percent reduction in thickness or areal density. The air space is 2.5 cm in both cases. In the energy range from 150 keV to 200 keV, near the peak of the surface energy deposition curve in Fig. 3, the ratios are within a few percent of unity. This indicates that the area throughput rate or line speed would be nearly insensitive to small changes in window thickness in this energy range. At 125 keV, the ratio shows an increase in the energy deposition of 13 percent, while at 100 keV, the increase is 43 percent. These increasing sensitivities as the electron energy decreases are consistent with the absorption of a larger fraction of the incident electron energy in the titanium window. The effects of a 20 percent reduction in window thickness would be less significant if the window were half as thick. Then it would have an areal density nearly the same as that of 2.5 cm of air⁷.

Table 2 gives comparisons of the surface values of the energy depositions per electron with two different air spaces. In one case, the air space is 2.5 cm and in the other case, the air space is 2.0 cm. This is a 20 percent reduction in thickness, which would be equivalent to a 20 percent reduction in air density at the same thickness. The titanium window is 15 μm in both cases. The air density is inversely proportional to the absolute temperature, so this reduction in density is equivalent to a temperature rise from 293 $^{\circ}\text{K}$ to 366 $^{\circ}\text{K}$ or from 20 $^{\circ}\text{C}$ to 93 $^{\circ}\text{C}$. In the energy range from 150 keV to 200 keV, which is near the peak of the surface energy deposition curve in Fig. 3, the ratios are within about 1.6 percent of unity. At 125 keV, the ratio shows an increase in the energy deposition of about 4 percent, while at 100 keV, the increase is about 14 percent. The effects of a 20 percent reduction in the air density are less significant than a 20 percent reduction in window thickness because the areal density of 2.5 cm of air is about half the areal density of 15 μm of titanium. This is evident from the depth-dose distributions in Figs. 1 and 2.

Table 1. Comparisons of the surface values of energy depositions for titanium thicknesses of 15 μm and 12 μm with an air space of 2.5 cm in each case.

Energy - keV	100	125	150	175	200
Ti - 15 μm	4.5194	7.3832	7.8987	7.5942	6.9757
Ti - 12 μm	6.4545	8.3174	8.2186	7.5412	6.7531
Ratio - 12/15	1.4282	1.1265	1.0405	0.9930	0.9681

Table 2. Comparisons of the surface values of energy depositions for air spaces of 2.5 cm and 2.0 cm with a titanium window thickness of 15 μm in each case.

Energy - keV	100	125	150	175	200
Air - 2.5 cm	4.5194	7.3832	7.8987	7.5942	6.9757
Air - 2.0 cm	5.1605	7.6768	8.0257	7.6284	6.9898
Ratio - 2.0/2.5	1.1419	1.0398	1.0161	1.0045	1.0020

Conclusion

The determination of absorbed dose with low-energy electron beams presents some challenges because of the shallow penetration of the electrons in dosimeters and irradiated materials. Calculations of absorbed energy using appropriate Monte Carlo codes can provide estimates of dose with sufficient accuracy for many industrial applications, provided that the input data describes the irradiation process realistically. Such calculations may also give more detailed information about dose distributions than can be obtained with thin film dosimeters, and they may be able to evaluate process conditions that are not attainable in a particular irradiation facility. This paper presents several examples to indicate how this method of analysis can supplement low-energy electron beam dosimetry.

References

1. D.E. Weiss, D.A. Cleghorn, S.V. Nablo, *Electron Beam Process Validation for Sterilization of Complex Geometries*, Radiat. Phys. Chem. **63** (2002) 581-586.
2. D.E. Weiss, *Electron Beam Tape Processing at Low Voltages*, at www.pstc.org/papers/abstracts/abstract-weiss.php (2004).
3. M. Cleland, R. Galloway, F. Genin, M. Lindholm, *The Use of Dose and Charge Distributions in Electron Beam Processing*, Radiat. Phys. Chem. **63** (2002) 729-733.
4. M.R. Cleland, T.F. Lisanti, R.A. Galloway, *Comparisons of Monte Carlo and ICRU Electron Energy vs. Range Equations*, Radiat. Phys. Chem. **71** (2004) 585-589.
5. T.F. Lisanti, *Calculating Electron Range Values Mathematically*, Radiat. Phys. Chem. **71** (2004) 581-584.
6. M.R. Cleland, R.A. Galloway, A.H. Heiss, J.R. Logar, , *Comparisons of Monte Carlo calculations with absorbed dose determinations in flat materials using high-current, energetic electron beams*, Nuclear Instr. Meth. Phys. Res., **B 261** (2007) 90-93.
7. M.R. Cleland, R.A. Galloway, A.J. Berejka, *Energy Dependence of Electron Beam Penetration, Area Throughput Rates and Electron Energy Utilization in the Low-Energy Region*, Nucl. Instr. Meth. Phys. Res. **B 261** (2007) 94-97.
8. M.R. Cleland, R.A. Galloway, *Dosimetry for Low-Energy Electron Beams*, Proceedings of the Eighth International Topical Meeting on Nuclear Applications and Utilization of Accelerators, AccApp'07, American Nuclear Society (2007) 686-691.
9. The International System of Units (SI), Ed. B.N. Taylor, Natl. Inst. Stand. Technol., **Spec. Publ. 330**, U.S. Gov. Printing Office, Washington, D.C. (1991).
10. J.A. Halbleib, R.P. Kensek, T.A. Mehlhorn, G.D. Valdez, S.M. Seltzer, M.G. Berger, "ITS Version 3.0, The Integrated TIGER Series of Coupled Electron/Photon Monte Carlo Transport Codes," SAND91-1634 (1992), CCC-467/ITS Code Package (1994). Available from the Radiation Safety Information Computational Center (RSICC), Oak Ridge, TN 37831, USA.
11. S.V. Nablo, *Electron-Beam Processing Machinery*, Chapter 9, Radiation Curing in Polymer Science and Technology, **Vol. 1** (Eds. J.P. Fouassier and J.F. Rabek), Elsevier Science Publishers Ltd. (1993).

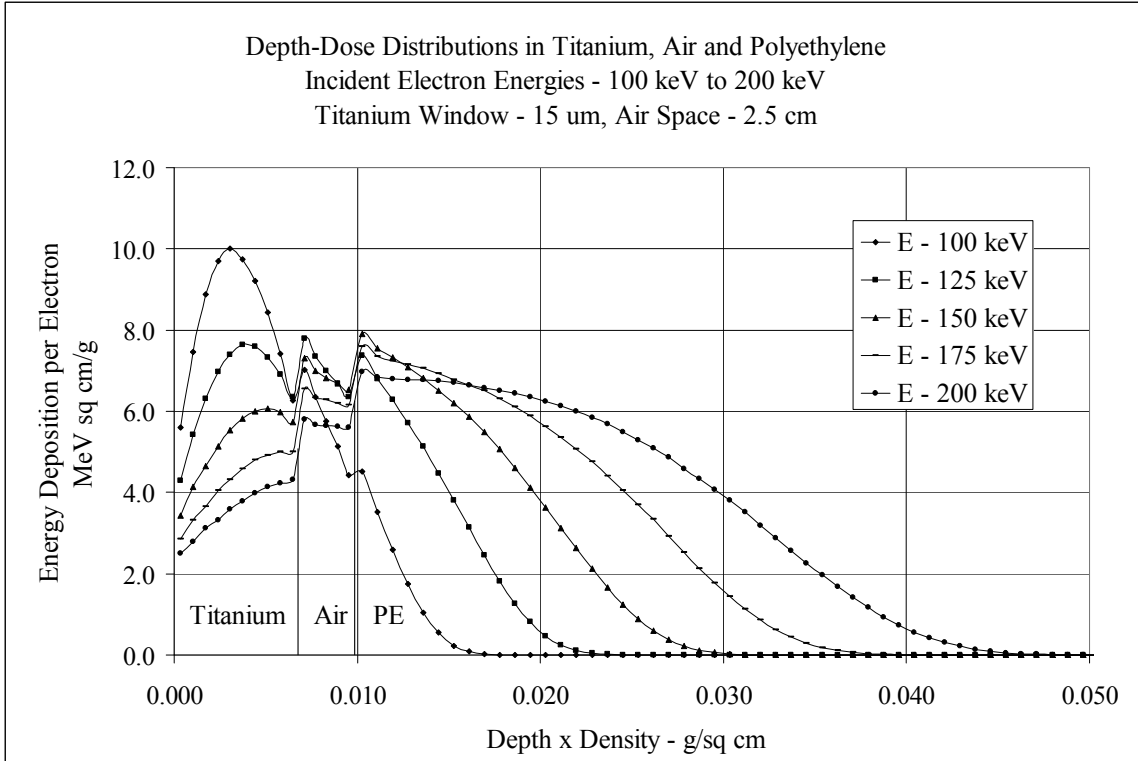


Fig. 1. Combined depth-dose distributions in titanium, air and polyethylene.

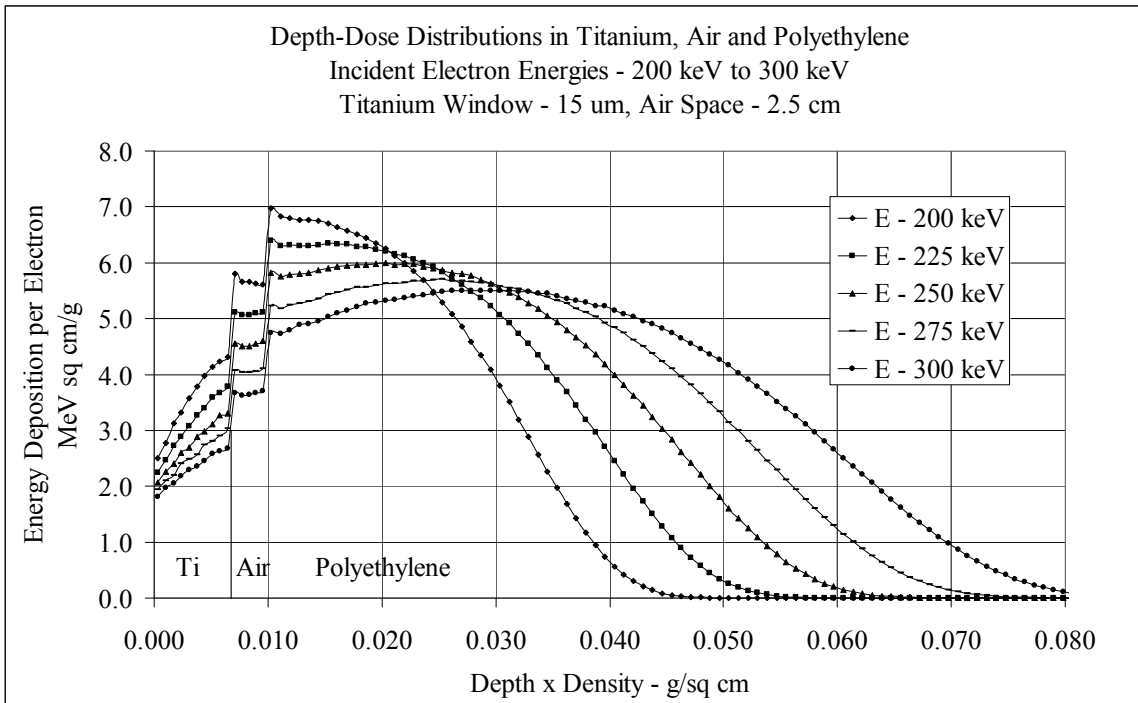


Fig. 2. Combined depth-dose distributions in titanium, air and polyethylene.

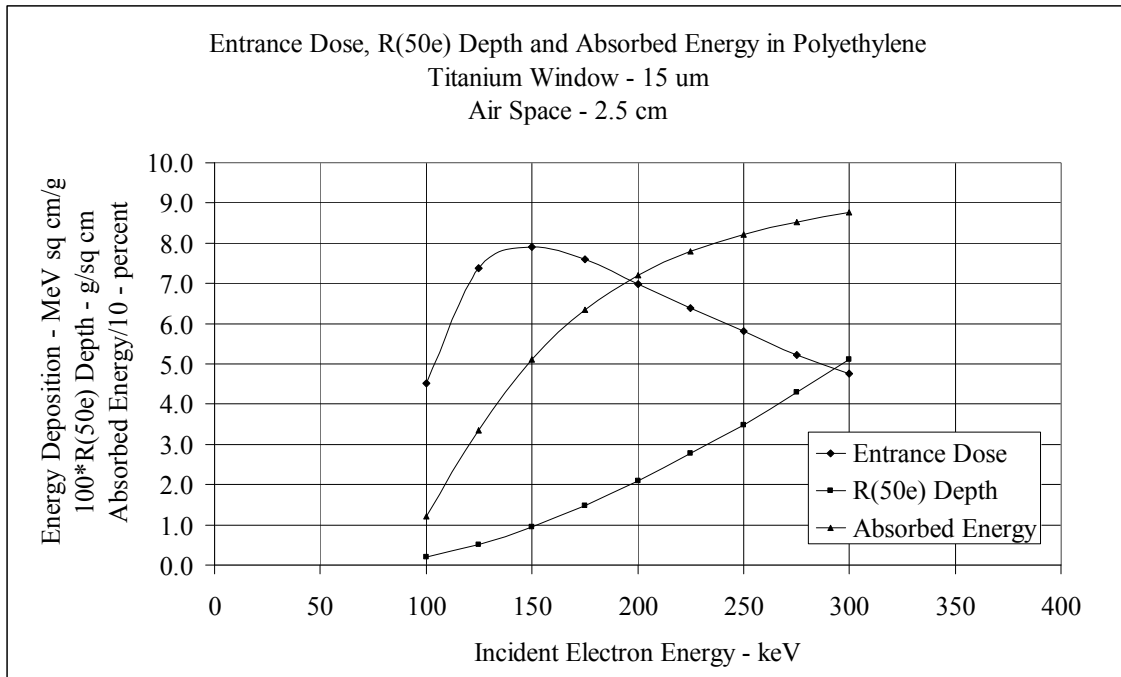


Fig. 3. Entrance dose, R(50e) depth and absorbed energy in polyethylene from 100 keV to 300 keV with a 2.5 cm air space.

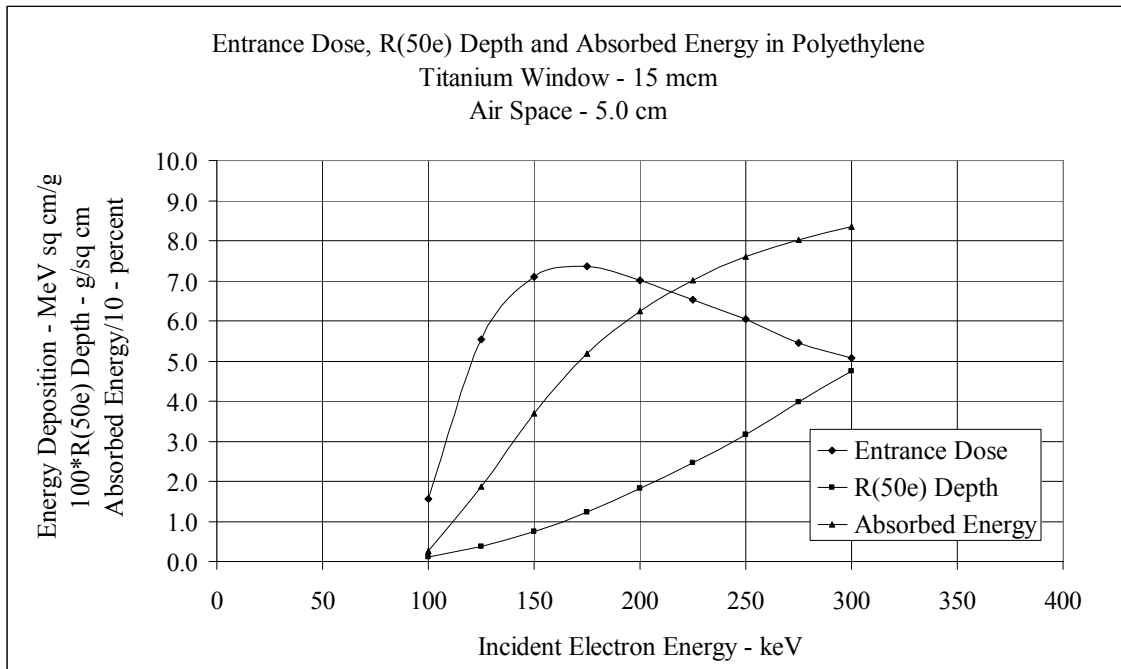


Fig. 4. Entrance dose, R(50e) depth and absorbed energy in polyethylene from 100 keV to 300 keV with a 5.0 cm air space.

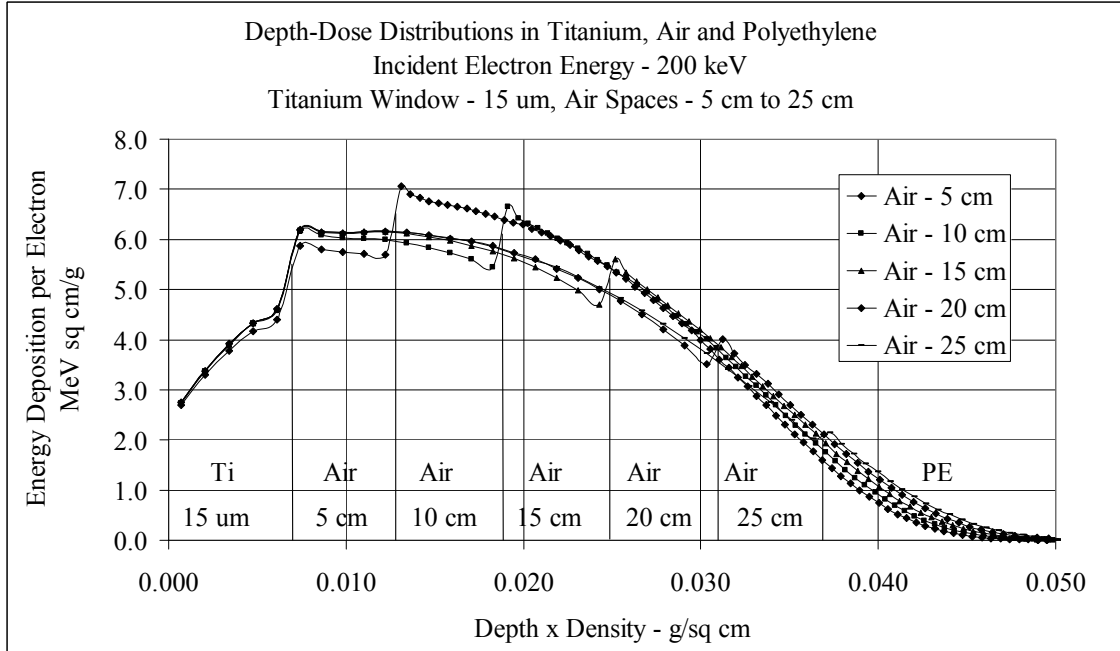


Fig. 5. Depth-dose distributions in titanium, air and polyethylene with air spaces of 5 cm, 10 cm, 15 cm, 20 cm and 25 cm at an energy of 200 keV.

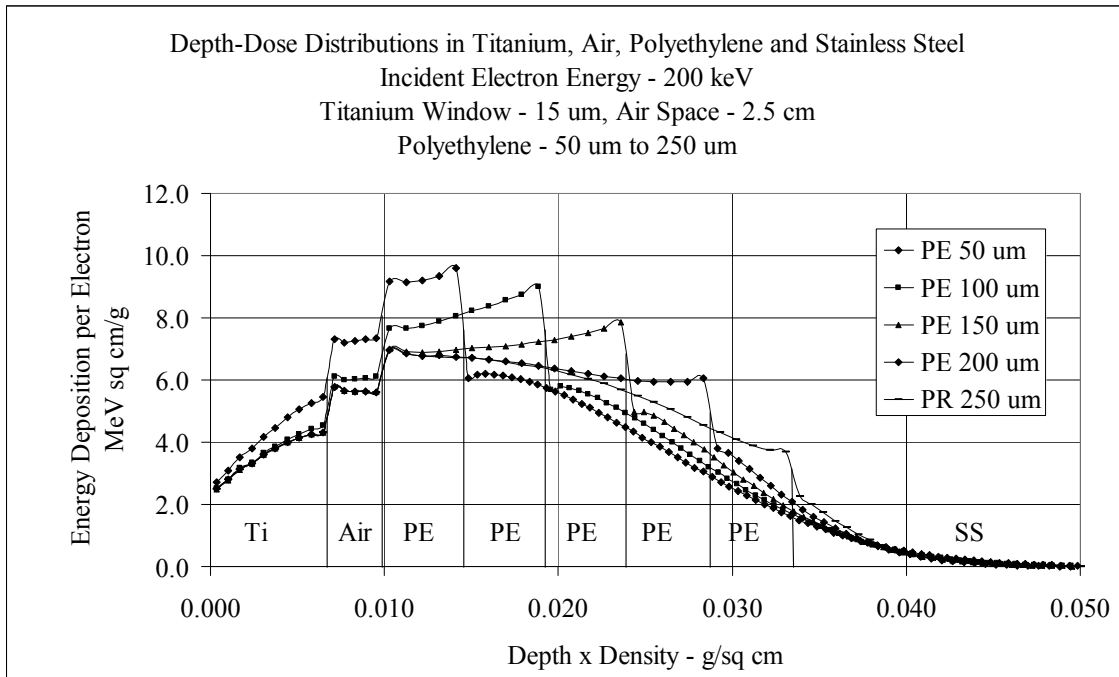


Fig. 6. Depth-dose distributions in titanium, air, polyethylene and stainless steel with polyethylene thicknesses of 50 μm , 100 μm , 150 μm , 200 μm and 250 μm at an energy of 200 keV.

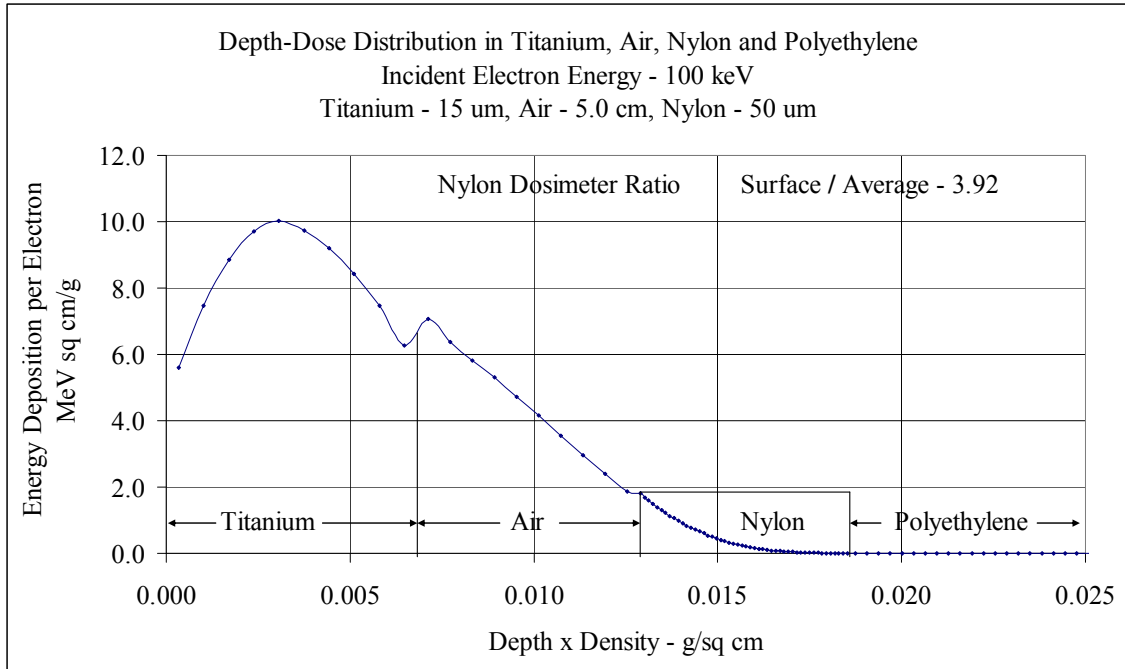


Fig. 7. Depth-dose distribution in titanium, air, nylon dosimeter and polyethylene at an energy of 100 keV. The ratio of surface to average dose in the nylon dosimeter is 3.92.

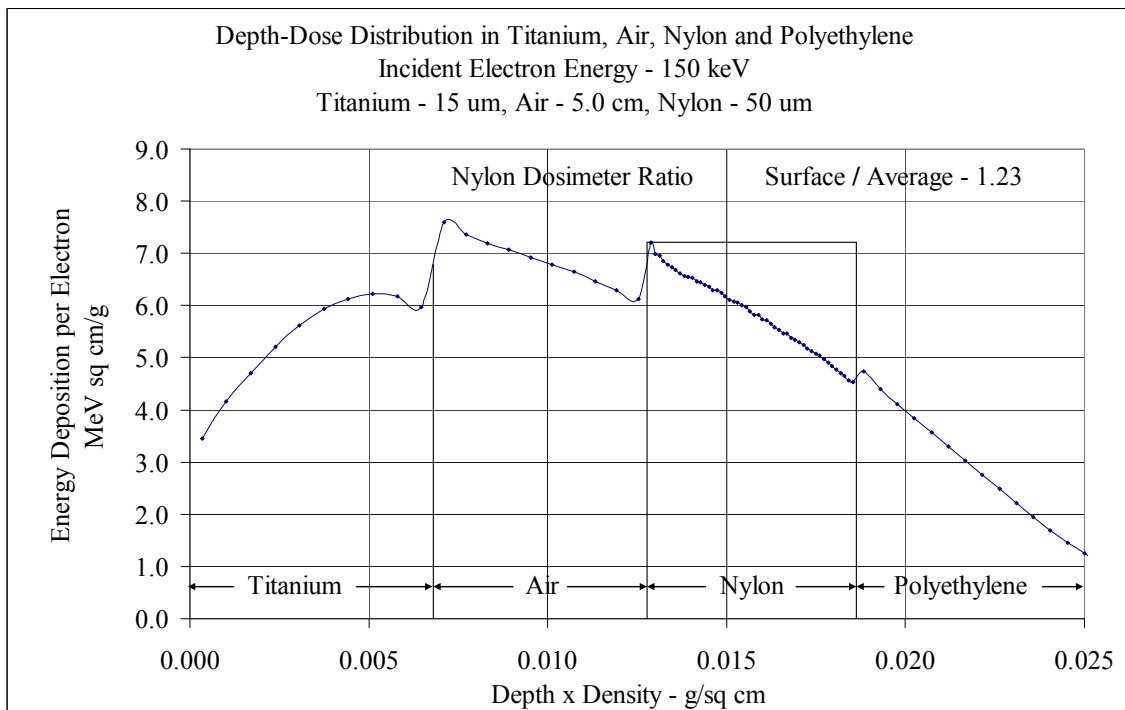


Fig. 8. Depth-dose distribution in titanium, air, nylon dosimeter and polyethylene at an energy of 150 keV. The ratio of surface to average dose in the nylon dosimeter is 1.23.

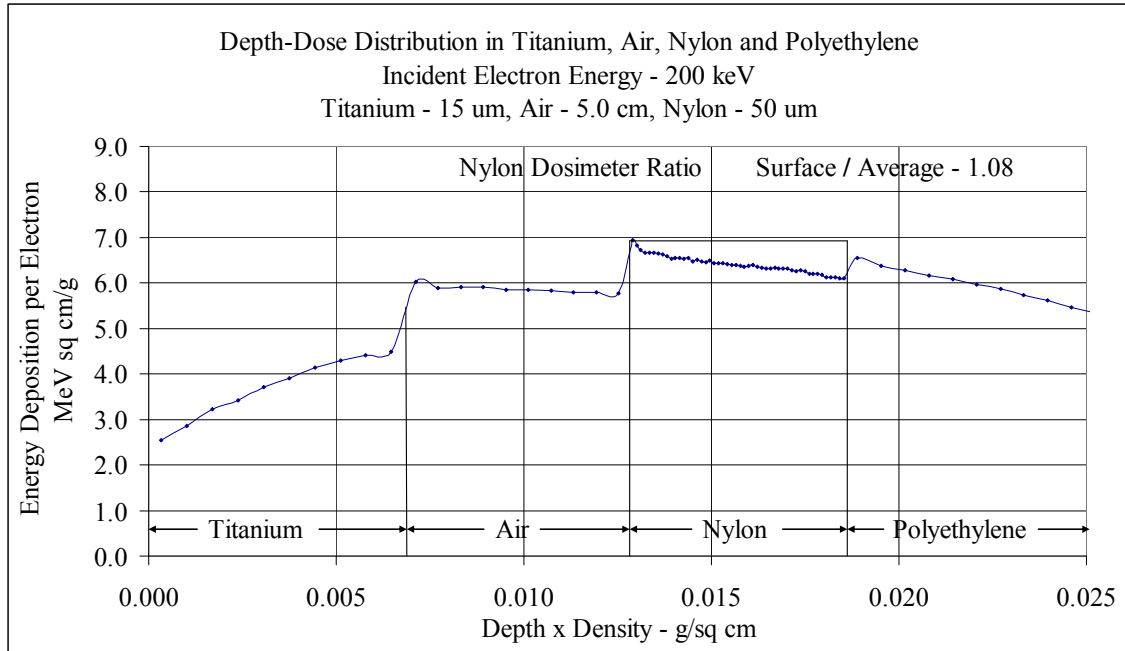


Fig. 9. Depth-dose distribution in titanium, air, nylon dosimeter and polyethylene at an energy of 200 keV. The ratio of surface to average dose in the nylon dosimeter is 1.08.

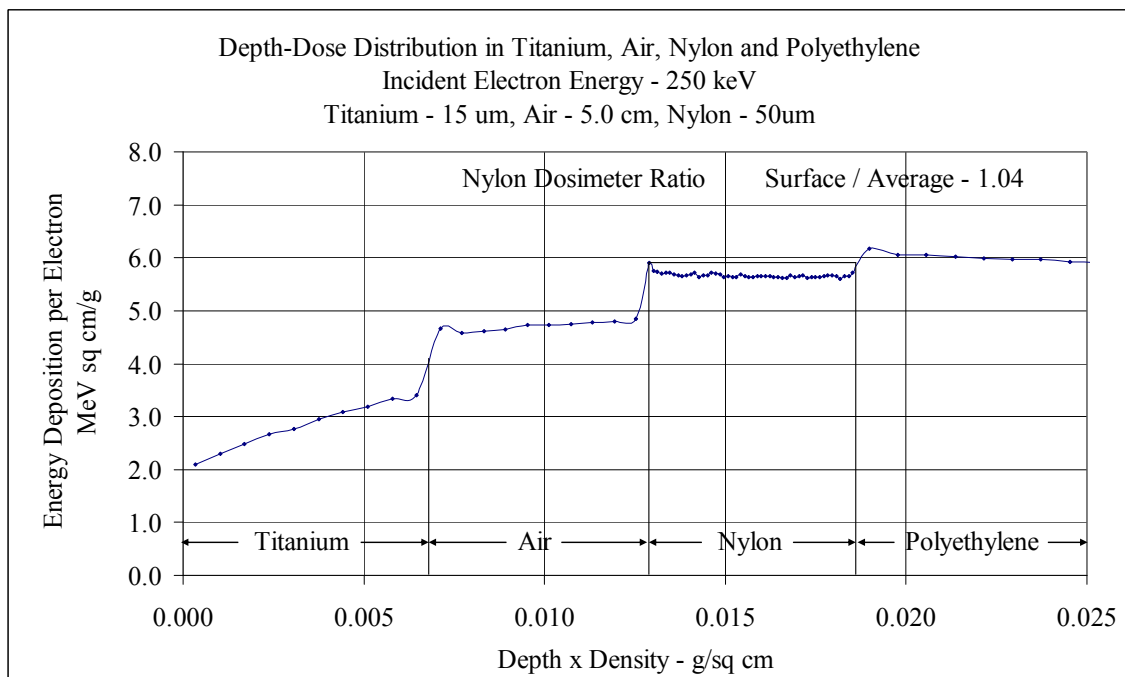


Fig. 10. Depth-dose distribution in titanium, air, nylon dosimeter and polyethylene at an energy of 250 keV. The ratio of surface to average dose in the nylon dosimeter is 1.04.